A transmission electron microscopy *in situ* study of dislocation mobility in Ge

2002 J. Phys.: Condens. Matter 14 12897

(http://iopscience.iop.org/0953-8984/14/48/330)

INSTITUTE OF PHYSICS PUBLISHING JOURNAL OF PHYSICS: CONDENSED MATTER

J. Phys.: Condens. Matter **14** (2002) 12897–12902 PII: S0953-8984(02)54092-3

A transmission electron microscopy *in situ* study of dislocation mobility in Ge

Tomas Kruml[1], **Daniel Caillard**[2], **Corinne Dupas**[1] **and Jean-Luc Martin**[1]

[1] IPMC, FSB, Ecole Polytechnique Fédérale de Lausanne, CH 1015 Lausanne, Switzerland
[2] CEMES—CNRS, Toulouse, France

E-mail: Tomas.Kruml@epfl.ch

Received 27 September 2002
Published 22 November 2002
Online at stacks.iop.org/JPhysCM/14/12897

Abstract
In situ deformation experiments were performed on pure Ge. In addition to qualitative observations being made, the velocity of dislocations was measured as a function of dislocation character and length at various temperatures and stresses. The local effective stress was estimated from the curvature of the dislocations. Combining the *in situ* results with double-etch-pit experiments allows estimation of the mean free path of kinks. Then a set of material parameters are calculated within the framework of the Hirth–Lothe theory.

M This article features online multimedia enhancements

1. Introduction

Transmission electron microscopy (TEM) *in situ* experiments are a powerful tool in the investigation of dislocation mobility in semiconductors (see reviews [1, 2] or a study on Si [3]). These experiments provide a unique way to observe the dislocation behaviour at the microscopic scale and can give hints as to which elementary processes control their mobility. However, a limited number of such results are available for Ge [4].

In covalent crystals, the velocity of short dislocations increases linearly with their length while that of long dislocations is expected to be length independent. The Hirth and Lothe (HL) kink diffusion theory [5] describes the details of the strong lattice resistance to glide in covalent crystals. The kink mean free path X controls the transition between the two dislocation velocity regimes and is therefore of prime interest.

2. Experiment

Pure $[\bar{1}23]$ Ge single crystals (single-slip orientation) are first predeformed in compression at 750 K in order to achieve a suitable initial dislocation density. The *in situ* specimens are cut from the predeformed block with the same stress axis and with the $(\bar{5}\bar{4}1)$ foil plane. The

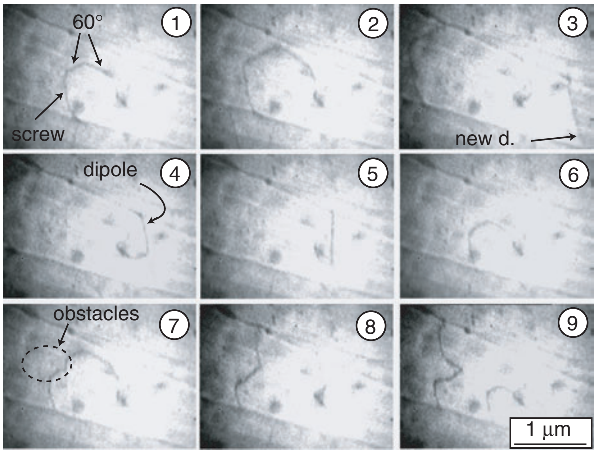

Figure 1. An example of a spiral source. 740 K.

active slip plane is thus inclined at 45° to the foil. The final chemical thinning is performed in an agent containing 27% HF, 46% HNO_3 and 27% CH_3COOH. The dislocation mobility is studied from 670 to 750 K. A JEOL 200 kV microscope is used.

3. Qualitative observations

3.1. General description

Dislocations gliding in the (111) primary plane tend to align along ⟨110⟩ Peierls valleys. This tendency increases with decreasing temperature. Primary dislocations are present with Burgers vector $(1/2)[\bar{1}01]$. The Schmid factors of the primary and secondary systems are 0.47 and 0.35 respectively. Numerous cross-slip events are observed in the case of the secondary system. The primary dislocations do not cross-slip, because of the zero Schmid factor on the cross-slip plane. Dislocation interactions, frequently leading to dipole formation or annihilation, are observed. A significant amount of dislocation debris in the form of small loops is present in the crystal after predeformation.

3.2. Sources

More than ten spiral dislocation sources, none being of the Frank–Read type, were observed. The Frank–Read source necessitates two strong pinning points, which are not likely to be present in a thin foil. The sources studied are not stable. They can originate from a dislocation interaction, move, escape from the foil or be destroyed by another dislocation interaction.

The sequence in figure 1 shows the hexagon-shaped segments emitted, in the first three frames. One 60° segment disappears at the surface in the third frame while another screw dislocation approaches from the right. The source screw segment and the new dislocation form a dipole in frames 4 and 5, which then annihilates and the lower part of the new dislocation is connected with the rest of the source in frame 6. The source continues to revolve (frames 7–9), but now multiplication takes place at the new dislocation. Surprisingly, its glide is perturbed by small invisible obstacles (below the resolution limit).

A spiral source of dissociated dislocations, which is assumed to be a twin source, is shown in figure 2. Since twins have never been observed in semiconductors in ‘post-mortem’ studies, it is believed to be a thin-foil artefact.

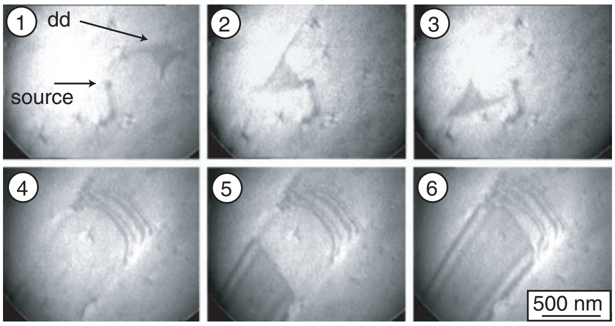

Figure 2. A source emitting dissociated dislocations (dd) (1, 2, 3) and a partial dislocation contributing to the twin (4, 5, 6). 693 K.

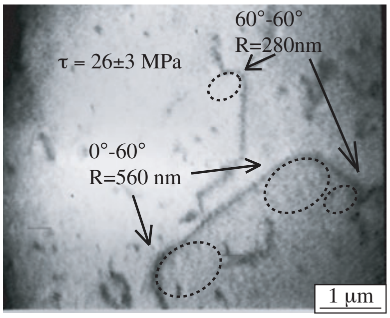

Figure 3. Measuring local stresses, 673 K.

4. Quantitative measurements

The aim is to measure dislocation velocities as a function of their character and length, as well as of the local stress. Therefore, the event studied must be carefully chosen. If the local stress is too small, dislocations may be slowed down by interactions with point defects. In particular, screw dislocations, less mobile than 60° ones, tend to be influenced by this effect. On the other hand, under high stresses, the curved part between the dislocation segments, used for the stress measurement, has too small a radius to be measured accurately.

In figure 3, a screw segment, about 2.5 μm long, is observed to be immobile; only two 60° segments are moving. The local stress τ is estimated as follows [6, 7]. Between the screw and 60° segments, the radius of curvature and stress are connected by the relation

$$\tau = \frac{1.328\mu b}{4\pi R_{60-0}} \ln\left(\frac{R_{60-0}}{2.9b}\right) \tag{1}$$

where R_{60-0} is the radius, b the Burgers vector, μ the shear modulus. The radius of curvature between two 60° segments is approximately half that in (1):

$$\tau = \frac{0.76\mu b}{4\pi R_{60-60}} \ln\left(\frac{R_{60-60}}{4.2b}\right). \tag{2}$$

In figure 3, the stress estimated in four areas, indicated by the arrows, is found to be 26 ± 3 MPa.

In the sequence of figure 4, the 60° dislocation is moving about twice as fast as the screw. As shown in figure 5, the velocities of the screw and 60° dislocations are found to be proportional to their respective lengths, with no indication of a slope change as the length

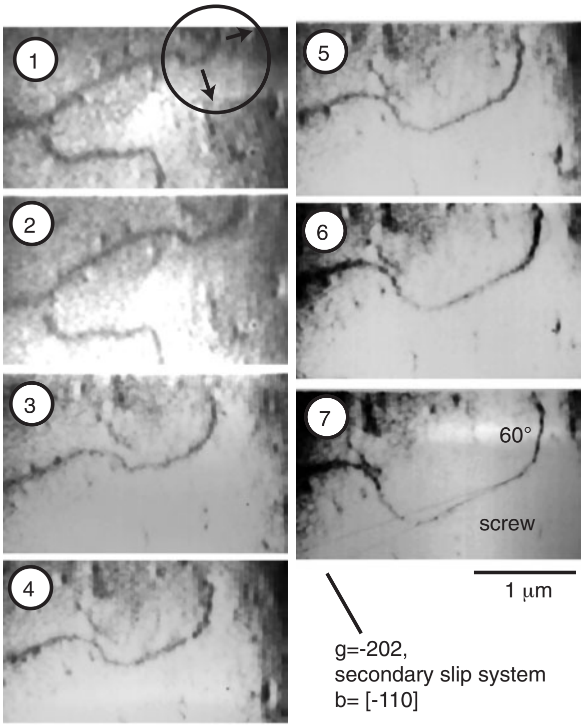

Figure 4. The effect of length on the velocity of a screw and a 60° dislocation 693 K.

increases. In contrast, Louchet *et al* [4] found a slowing down of dislocations for a length of about 1 μm. They estimated the velocity v_∞ in the length-independent regime using an extrapolation procedure. In the present study, velocity measurements at various temperatures and stresses never showed any evidence of the length-independent regime. It is worth noting that due to the limited foil thickness, the interval of dislocation length investigated has an upper limit of about 1.5 μm.

Therefore, independent measurements of dislocation velocities by double-etch-pit experiments, performed on the same material, are considered [8]. Indeed, the dislocation length is expected to correspond to the length-independent regime. The velocity of screw dislocations was found to follow relation (3) for the interval of stresses investigated, 10–50 MPa, at 750 K [8]:

$$v_\infty = 16.2(\tau/\mu)^{2.09}. \tag{3}$$

Since the measurements are performed with a very low initial dislocation density, the applied stress is considered to be close to the local stress.

The mean free path of kinks X is then estimated using relation (4):

$$X = \frac{v_\infty}{2(\partial v/\partial L)}. \tag{4}$$

The slope $\partial v/\partial L$ is measured on a curve similar to that of figure 5, obtained from an *in situ* observation at a given stress. v_∞ is provided by relation (3) for that stress. X is estimated using relation (4), for three events at 750 K. The values are presented in table 1.

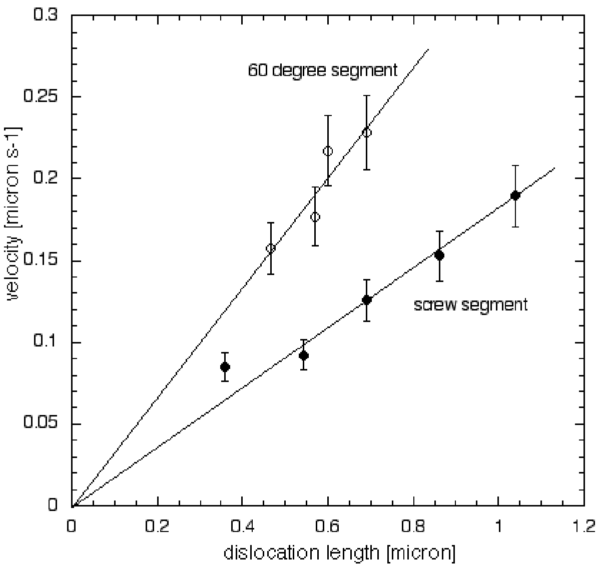

Figure 5. Velocity data corresponding to figure 4.

Table 1. Parameters of the HL theory deduced from the *in situ* observations; $T = 750$ K.

τ (MPa)	X (μm)	$\partial v/\partial L$ (s^{-1})	v_∞ ($\mu m\ s^{-1}$)	P_{kp} ($m^{-1}\ s^{-1}$)	v_k ($\mu m\ s^{-1}$)	U_{ik} (eV)	U_m (eV)	U_k (eV)	ΔG, $L \ll X$ (eV)	ΔG, $L \gg X$ (eV)
50	4.9	0.66	6.5	3.3×10^9	26 000	1.13	0.73	0.67	1.86	1.30
40	6.7	0.36	4.8	1.8×10^9	26 700	1.17	0.72	0.68	1.89	1.31
35	4.7	0.36	3.4	1.8×10^9	13 400	1.12	0.76	0.65	1.88	1.32

5. Comparison with the Hirth and Lothe kink diffusion theory

In this section, a set of dislocation mobility parameters are calculated within the framework of the theory [5]. The formulae and notation used here follow the recently revisited version [9], which differs slightly from the original treatment and where the following quantities are defined. An estimation of X is necessary prior to their calculations. Three events at 750 K, where X and the local stress were measured simultaneously, are analysed, considering the following quantities.

(i) The net kink-pair nucleation rate per unit dislocation length P_{kp}:

$$P_{kp} = \frac{v_\infty}{hX} \tag{5}$$

where h is the distance between two secondary Peierls minima in the $\langle 112\rangle$ direction, i.e.

$$h = \frac{\sqrt{3}}{2}b. \tag{6}$$

(ii) The kink velocity v_k:

$$v_k = \frac{1}{P_{kp}}\left(\frac{v_\infty}{2h}\right)^2. \tag{7}$$

(iii) The energy of the double-kink nucleation U_{ik}. This is related to X by

$$X = 2b\exp\left(\frac{U_{ik}}{2kT}\right). \tag{8}$$

The activation energy ΔG of the dislocation velocity is different in the length-dependent and length-independent regimes.

(iv) ΔG in the length-dependent regime. Relations (9) and (10) are valid:

$$\Delta G = U_{ik} + U_m, \tag{9}$$

$$v = \nu_D \frac{\tau h^2 b}{kT} L \exp\left(-\frac{U_{ik} + U_m}{kT}\right) \tag{10}$$

where ν_D is the Debye frequency (0.91×10^{13} s^{-1} for Ge) and τ is the local stress. ΔG can thus be experimentally determined, extracting the derivative $\partial v/\partial L$ from the *in situ* measurements and using equation (10).

(v) The energy of kink migration U_m. This is calculated from (9), U_{ik} being known from (8).

(vi) ΔG in the length-independent regime:

$$\Delta G = \tfrac{1}{2}U_{ik} + U_m. \tag{11}$$

Finally, (vii) the single-kink formation energy U_k. This is given by

$$U_{ik} = 2U_k - hb\left(\frac{hb}{2\pi}\mu\tau\right)^{1/2}. \tag{12}$$

The results are summarized in table 1.

6. Discussion and conclusions

The stress exponent m of the velocity, in the length-dependent regime, can be estimated from the first and the third columns of table 1, in spite of some experimental scatter. The value of $m = 2 \pm 0.5$ is found. The agreement with the measured m-value in the length-independent regime (relation (3)) is quite striking (same temperature). This fact reminds us of a previous result [10] concerning activation energies of the velocity which were found to be the same in the length-dependent and length-independent regimes. This was interpreted by the authors by considering that the glide of long dislocations in the bulk crystal is *not* in the kink collision regime—on the contrary, the saturated velocity would be dictated by the presence of obstacles, which hinder kink propagation.

Work is in progress to check this interpretation further and to extend the measurements of table 1.

References

[1] Louchet F and George A 1983 *J. Physique* C **4** 51
[2] Vanderschaeve G, Levade C and Caillard D 2001 *J. Microsc.* **203** 72
[3] Louchet F 1981 *Phil. Mag.* A **43** 1289
[4] Louchet F, Cochet Muchy D, Brechet Y and Pelissier J 1988 *Phil. Mag.* A **57** 327
[5] Hirth J P and Lothe J 1992 *Theory of Dislocations* (Malabar, FL: Krieger) p 531
[6] Gottschalk H 1983 *J. Physique* **44** C4 69
[7] Fnaiech M, Reynaud F, Couret A and Caillard D 1987 *Phil. Mag.* A **55** 405
[8] Dupas C, Zuodar N, Coddet O, Kruml T and Martin J L 2002 *J. Phys.: Condens. Matter*
[9] Caillard D and Martin J L 2002 *Thermally Activated Dislocation Mechanisms of Crystal Plasticity* (Amsterdam: Elsevier) at press
[10] Maeda K and Takeuchi S 1996 *Dislocation in Solids* vol 10 (Amsterdam: Elsevier) p 443